Tumor Biol. (2012) 33:1179–1189
DOI 10.1007/s13277-012-0363-x

RESEARCH ARTICLE

Natural withanolide withaferin A induces apoptosis in uveal melanoma cells by suppression of Akt and c-MET activation

Abbas K. Samadi · Stephanie M. Cohen · Ridhwi Mukerji · Vamsee Chaguturu · Xuan Zhang · Barbara N. Timmermann · Mark S. Cohen · Erica A. Person

Received: 26 December 2011 / Accepted: 13 February 2012 / Published online: 5 April 2012

Abstract Uveal melanoma (UM) is the most common primary intraocular malignancy in adults. While effective therapy exists for the primary tumor, there is a lack of effective treatment for metastatic disease currently. Natural withanolide withaferin A (WA) has shown efficacy in cancers demonstrating upregulation of pro-survival pathways. The purpose of the present study is to investigate the effect of WA as a potential therapeutic agent for UM in vitro as well as in vivo. UM cells were treated with WA and several cell-based assays, such as MTS, trypan blue exclusion assay, clonogenic, wound healing, cell cycle shift, annexin V/propidium iodide, and Western blot, were performed. In vivo experiments utilized the 92.1 cells in a xenograft murine model. WA inhibits cell proliferation of uveal melanoma cells with an IC50 of 0.90, 1.66, and 2.42 μM for OMM2.3, 92.1, and MEL290 cells, respectively. Flow cytometry analysis demonstrates G2/M cell cycle arrest and apoptosis at 1 μM WA in treated cells. WA induced apoptosis partly through the suppression of c-Met, Akt, and Raf-1 signaling activation. In vivo studies using WA reduced tumor growth in 100% of animals (p=0.015). Our observation indicates that WA is a potent drug that inhibits cell proliferation, shifts cell cycle arrest, and induces apoptosis in multiple UM cell lines in vitro. WA-mediated apoptosis in UM cells is partly mediated though the suppression of c-Met and Akt activation. WA significantly decreases UM tumor growth in vivo and justifies further evaluation of this drug for the treatment of metastatic uveal melanoma.

Keywords Uveal melanoma · Withaferin A · Apoptosis · Cell cycle arrest · c-Met inhibition

E. A. Person
Department of Ophthalmology, School of Medicine,
University of Kansas Medical Center,
Kansas City, KS, USA
e-mail: eperson@kumc.edu

A. K. Samadi (✉) · S. M. Cohen · R. Mukerji · V. Chaguturu · X. Zhang · M. S. Cohen
Department of Surgery, University of Kansas Medical Center,
Kansas City, KS, USA
e-mail: asamadi@kumc.edu

B. N. Timmermann
Department of Medicinal Chemistry, University of Kansas,
Lawrence, KS, USA

Introduction

Uveal melanoma (UM) is the most common primary intraocular malignancy in adults with an annual incidence of 8.4–11.7 cases per million population. It arises from melanocytes of the choroid, ciliary body, or iris of the eye and has a high propensity to metastasize to the liver [1, 2]. UM is a devastating and fatal disease once metastasis occurs. While multiple therapies have been evaluated to treat this metastatic disease, none have achieved satisfactory results to date justifying the need for novel therapies.

Withaferin A (Fig. 1a) is a novel steroidal lactone present in *Withania somnifera*, a plant described in Ayurvedic medicine in India for centuries and used to enhance health and treat a variety of gastrointestinal and arthritic ailments [3, 4]. In the past decade, WA has been shown to have anti-cancer activity against several cancer types including leukemia, colon, pancreas, breast, thyroid, oral squamous cell cancer, glioblastoma, and cutaneous melanoma [5–10]. WA has the ability to inhibit multiple targets important for UM tumor survival, including c-

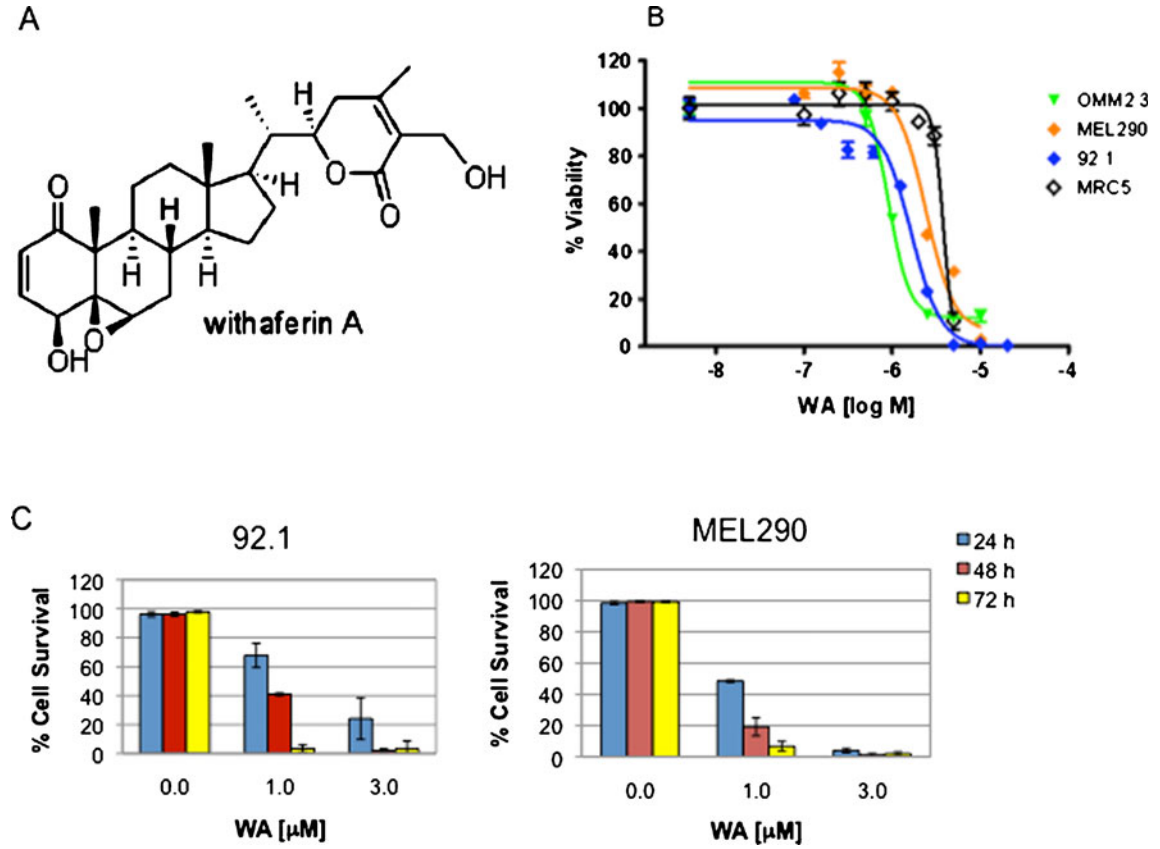

Fig. 1 Growth inhibition of uveal melanoma cells by *WA*. **a** Chemical structure of withaferin A is presented. **b** Cells were incubated with or without WA at various concentrations for 72 h, and viability was determined by MTS assay. Viability was calculated relative to time-matched untreated controls. **c** Trypan blue exclusion assay was performed with increasing concentrations of WA in 92.1 and MEL290 cells for 24, 48, and 72 h. Experiments carried out in triplicate were averaged with mean±SD

MET, the phosphatidylinositol 3-kinase (PI3K)/Akt pathway, and the MAP kinase pathway. Similar to cutaneous melanoma, constitutive ERK1/2 activation has been documented in primary UM tumors and cell lines even though, unlike cutaneous melanoma, they express both ^{WT}Ras and ^{WT}B-Raf [11–13]. B-Raf silencing or small molecular inhibitors of B-Raf reduced ERK1/2 activation and reduced cell proliferation and transformation in both ^{WT}B-Raf and ^{V600E}B-Raf UM cell lines [14]. These findings underline the importance of the MAP kinase signaling pathway in UM. Other activated pro-survival signaling pathway(s) cooperate with B-Raf to induce the cancerous state [15]. The proliferative effects of the B-Raf activation may be complemented by the antiapoptotic signals of the PI3K/Akt pathway. It has been observed that the autocrine stem cell factor-dependent activation of c-Kit induces ERK1/2 as well as PI3K/AKT activation in UM cell lines [16]. Furthermore, activated RAS also triggers the activation of PI3K/AKT pathway, which complements the proliferative effects of the ERK pathway [17].

Screening of potential oncogenes that may activate the MAP kinase pathway has led to the discovery of mutations in GNAQ, a stimulatory α_q subunit of heterotrimeric G proteins (alpha Q/11) found in UM primary cells [18, 19]. Constitutive activation of GNAQ promotes activation of calcium-dependent protein kinase C, which in turn, stimulates the RAF/MEK/ERK pathway. The activated G-protein also stimulates the PI3K/Akt pathway, which converges with the MAP kinase pathway to activate cyclin D and perpetuate the cell cycle [20]. Furthermore, recent reports indicate that the expression of c-Met and its ligand hepatocyte growth factor (HGF) are associated with tumor growth in the liver and liver metastasis of UM [21–24]. c-Met is a receptor tyrosine kinase for HGF and leads to activation of multiple downstream signaling pathways including the Ras protein kinase and PI3Kinase/Akt pathway [25, 26]. Additionally, PTEN, a dual-specificity phosphatase that blocks activation of the Akt pathway, is frequently downregulated in UM leading to the activation of PI3kinase/Akt pro-survival pathway [27]. Since phosphorylated Akt blocks apoptosis and is associated with negative prognostic indicators in patients with UM, targeting PI3kinase/Akt signaling pathway may be a viable option for inhibition of growth and metastasis of UM [20, 28].

Targeted inhibition of the components of the MAP kinase pathway has produced disappointing results in UM cells. B-Raf mutant UM cells undergo cell cycle arrest but not apoptosis upon treatment with the specific B-Raf inhibitor AZD6244 or the MEK inhibitor PLX4720 [29]. Additionally, UM cells bearing Gα-protein mutation (GNAQ or GN11) were mildly sensitive to AZD6244 but completely resistant to PLX4720. Paradoxically, ERK1/2 is activated upon treatment with PLX4720 in Gα-mutant UM cells. The combination treatment with AZD6244 and PLX4720 synergistically inhibited growth of B-Raf mutant UM cells, while this combination had little effect on Gα-mutant UM cells [29]. PI3K inhibition by LY294002 in B-Raf mutant UM cells significantly reduced cell proliferation [30]. Furthermore the Akt inhibitor MK2206 sensitized B-Raf-mutant cells to both PLX4720 and AZD6244 and sensitized Gα-mutant cells to AZD6244, but it could not overcome the resistance of the Gα-mutant cells to PLX4720 [29]. These studies thus suggest that the response of UM cells to inhibition of B-Raf, MEK, and Akt depends somewhat on their genotype. Additionally, targeted B-Raf or MEK inhibition alone may not be sufficient for the treatment of UM, and inhibition of other activated pro-survival targets including PI3K/Akt may be required for the effective treatment of UM either as a single agent or in combination therapy.

The objective of the current study, therefore, is to explore the activity of WA on uveal melanomas in vitro related to its effects on cell proliferation and viability, cell cycle modulation, induction of apoptosis, and modulation of the c-Met and PI3Kinase/Akt, as well as in vivo effects on UM tumor growth in a murine xenograft model of UM.

Material and methods

Cell culture growth

Three human uveal melanoma cell lines including OMM2.3 and MEL290 cells (kindly provided by Dr. JW Harbour, Washington University, St. Louis, MO), 92.1 cells (obtained with permission from Martine J. Jager, Leiden University, The Netherlands; and kindly provided by Dr. Jerry Neiderkorn), and normal human fetal fibroblast MRC-5 cells (obtained from American Type Culture Collection, Manassas, VA) were used for in vitro experiments. UM cells were propagated in RPMI supplemented with 10% heat inactivated fetal bovine serum (FBS) and 1% penicillin–streptomycin at 37°C in a humidified 5% CO_2-enriched atmosphere. MRC-5 cells were propagated in DMEM supplemented with 10% FBS and 1% penicillin–streptomycin. WA was purchased from Chromadex (Irvine, CA) and was dissolved in DMSO at 20 mM stock concentration. Cells were treated with WA at indicated concentrations.

Cell proliferation assay

The cell proliferation assay was performed in triplicate on 96-well plates (2×10^3 cells/well). Cells were plated overnight and WA was added with ten serial dilutions, ranging from 20 to 0.075 μM and incubated at 37°C for 72 h. Cell viability was then assessed using CellTiter 96 AQueous One assay (Promega, Madison, WI) according to the manufacturer's protocol. The absorbance was obtained at 490 nm by spectrophotometry (BioTek Synergy 2, Winooski, VT). DMSO at 0.01% was used as control in all in vitro experiments. A non-malignant control cell line evaluation was performed using MRC-5 cells at 2×10^3 cells/well over the same range of WA concentrations. IC50s were calculated and plotted using GraphPad Prism 5 software (GraphPad Software, La Jolla, CA). To confirm the MTS cell viability assay, a trypan blue exclusion assay was performed. After 24 h of treatment, the cells were stained with trypan blue dye and counted to determine the total number of viable cells. The percent of cell survival was calculated by comparison of stained and unstained cells.

Colony formation assay

UM cells were seeded into 60 mm plates (500 cells/plate) and allowed to grow overnight. The cells were then incubated in the presence or absence of multiple concentrations of WA for 24 h. The WA-containing medium was then removed, and the cells were washed with 1× phosphate-buffered saline (PBS) and incubated for an additional 10 days in complete medium without WA. Media was removed and fresh media was added every 3 days. The colonies obtained were washed with 1×PBS and fixed in coomassie blue–methanol solution for 20 min at room temperature. The colonies were washed and photo-documented. Each treatment was performed in triplicate.

Cell migration assay

UM cells were initially grown to confluence on 60 mm tissue culture plates, then a central linear area was cleared using a sterile micropipette tip. Floating cells were removed by washing with 1× PBS. Cell migration back into the cleared area was observed after incubation with multiple concentrations of WA for over a 48-h period. Cells were photographed using a phase-contrast microscope.

Cell cycle analysis

To perform cell cycle analysis on flow cytometry, UM cells were treated with 0, 1.0, 2.5, and 5.0 μM for 24 h. Cells were trypsinized and washed with 1× PBS and suspended in 1× PBS. Ethanol was added to a final concentration of 70% and stored at −20°C overnight. Cells were then washed with

1× PBS to remove ethanol and suspended in PBS containing 0.25 mg/mL DNase free RNase (Sigma-Aldrich, St. Louis, MO). After nuclei staining with propidium iodide (PI, 50 μg/mL; Sigma-Aldrich, St. Louis, MO) in the dark at room temperature, flow cytometry was performed using FACS/Calibur analyzer (BD LSRII; Becton Dickinson, San Diego, CA) capturing 10,000 events for each sample. Data from three identical analyses were used to confirm the results.

Assessment of apoptosis by annexin V/propidium iodide

Apoptotic analysis of UM cells treated with WA was accomplished by annexin V/PI staining and flow cytometry analysis. After treatment, cells (1×10^6 cells/mL) were washed with 1× PBS, and trypsinized. Cells were then stained with annexin V/PI according to the manufacturer's instruction (BD Bioscience; San Diego, CA) and were analyzed by flow cytometry. Apoptosis was then confirmed on Western blot analysis.

Western blot analysis

After treatment with WA at concentrations ranging from 0 to 5.0 μM, cells were lysed on ice with lysis buffer: 20 mM Tris; pH 7.4, 150 mM NaCl, 1 mM EDTA, 1% Triton X-100, 0.1% SDS, 0.25% sodium deoxycholate, 1 mM PMSF, 1 mM NaF, 1 mM dithiothreitol, 1 mM sodium orthovanadate, 1× protease inhibitor (Sigma-Aldrich, St. Louis, MO). Cell lysates were incubated on ice for 30 min and centrifuged at 14,000 rpm for 15 min at 4°C. Protein concentration was determined by BCA protein assay kit (Pierce Chemical Co., Rockford, IL). Equal amount of proteins (15–50 μg) were applied to 8–12% gels and subjected to SDS-PAGE. The samples were then transferred to a nitrocellulose membrane (Hybond; Amersham Biosciences Inc., Arlington Heights, IL) for 1 h. Membranes were blocked for 1 h at room temperature with 5% dry milk in PBS and incubated overnight at 4°C with primary antibodies against phospho-Akt, Ser473 (1:1,000), Akt (1:1,000), phospho-c-MET (1:2,000), c-MET (1:1,000), anti-RAF-1 (1:1,000), caspase-3 (1:1,000), and anti-PARP (1:1,000), (Cell Signaling, Beverly, MA), and anti-actin (1:50,000) (Millipore, Billerica, MA). All secondary antibodies were purchased from Santa Cruz Biotechnology Inc. (Santa Cruz, CA). Membranes were washed and incubated with 1:5,000 anti-mouse or anti-rabbit IgG conjugated to horseradish peroxidase for 1 h at room temperature and washed again. Signals were visualized using chemiluminesence reagents (Pierce Chemical Co., Rockford, IL). Beta-actin served as a loading control.

Murine in vivo model

Five-week-old female SCID mice weighing approximately 20–25 g (Charles River Laboratories, Wilmington, MA) were used for the in vivo experiment. Twenty-four mice were injected in the right flank with 92.1 cells (3.5×10^6 cells/animal) suspended in 1× PBS. Tumors were monitored for growth over a 2-week period and measured three times weekly for growth using a digital caliper. When tumors reached a minimum diameter of 3 mm in one dimension, the mice were randomized into one of three treatment groups: control (saline, no drug), 8 mg/kg/day WA, or 12 mg/kg/day WA ($N=8$ per group). Animals were injected intraperitoneally with WA or control daily for 21 days and then observed for an additional 4 weeks. One mouse from each group was sacrificed at the end of the 21-day treatment period for organ and tumor mass analysis. Final $N=7$ for statistical analysis. Tumor measurements and monitoring for overall health (weight loss or body score) was performed three times weekly during this period in accordance with our approved animal care and use protocol and the ARVO use of animals in Ophthalmic and Visual Research. Mice were sacrificed if criteria for morbidity were met or at the end of the study period. Primary tumors along with major organs (kidney, liver, spleen, bone marrow, injection site, brain, lungs, and heart) were harvested for additional testing and histologic evaluation.

Statistical analysis

All in vitro experiments were repeated in triplicate, and all in vivo data and assays were analyzed using GraphPad Prism 5.0 software (GraphPad Software, Inc., La Jolla, CA) and SPSS Statistics 17.0 (SPSS, Inc., Chicago IL). Differences between two or more means were determined by Student's unpaired t test (2 means) or one-way ANOVA followed by Duncan's multiple range test (2+ means). The level of significance was set at $p<0.05$.

Results

Effect of WA on proliferation of uveal melanoma cells

Using the MTS assay, WA reduced cell viability in multiple UM cell lines with an IC50 of 0.90, 1.66, and 2.42 μM in OMM2.3, 92.1, and MEL290 cells, respectively. MRC-5 fibroblast cells were used as a non-malignant control and exhibited an IC50 level with WA treatment of 3.81 μM (Fig. 1b). Cytologic features of cell injury in the form of cytoplasmic vacuoles were seen in WA-treated UM cell lines starting from 1.0 μM WA and were most prominent in the 92.1 and MEL290 cell lines. Cytologic features of cell death including cellular shrinkage, pyknosis, karyorrhexis, and karyolysis were observed in all cell lines at concentrations above 3.0 μM (data not shown). Subsequent studies were carried out using 92.1 and

MEL290 cells to determine the differential sensitivity of these cells to WA treatment. Trypan blue exclusion analysis showed that WA reduced cell proliferation of 92.1 and MEL290 cells in both concentration- and time-dependent manner (Fig. 1c). Cell survival decreased from 48.6±0.7% to 19.2±5.8% to 6.7±3.1% for MEL290 cells at 1.0 μM WA for 24, 48, and 72 h time points, respectively. Similarly, 92.1 cell survival decreased from 67.8±8.2% to 40.9±0.9% to 3.4 ±2.4% at 1 μM WA for 24, 48, and 72 h time interval, respectively ($p<0.05$ for all time points compared to the control for MEL290 and 92.1 cells). When the concentration of WA was increased to 3.0 μM, a substantial decrease in cell viability was noted in both MEL290 and 92.1 cells as early as 24 h. When MEL290 cells were treated with 3.0 μM WA, cell survival decreased to 4.0±1.4% to 1.1±0.8% to 2.0±1.2% for 24, 48, and 72 h time points, respectively. Similarly, treatment of 92.1 cells with 3.0 μM WA reduced cell survival to 24.1±14.3% to 2.0±1.3%, and to 3.1±2.5% for 24-, 48-, and 72-h time intervals respectively ($p<$ 0.001 for all time points compared to the control for MEL290 and 92.1 cells).

Colony formation of UM cells treated with WA

To measure long-term effects of WA on permanent cell growth arrest and cell death, we performed clonogenic survival assays. Clonal growth of 92.1 and MEL290 cells were suppressed by WA treatment. WA at 400 nM significantly reduced colony formation in both UM cell lines (Fig. 2a).

Cell migration of UM cells treated with WA

WA suppressed 92.1 UM cell migration for 24 and 48 h in a concentration-dependent manner. Cell migration was inhibited at 100 nM concentration of WA after 24 h and at 600 nM of WA at 48 h of treatment. Similarly, WA reduced MEL290 cell migration at 4.0 μM after a 12-h treatment (Fig. 2b). MEL290 cells were noted to migrate more rapidly compared to the 92.1 cells and required a greater concentration of WA to suppress cell migration.

The effect of WA on the cell cycle in uveal melanoma cells

Treatment of UM with WA induced a shift of cell cycle arrest with enhanced G_2/M and S phase arrest following treatment in a concentration-dependent manner in MEL290 and 92.1 cells. Vehicle only treated with 92.1 cells show a typical pattern of randomly cycling cells distributed across the G_1 (57.4%), S (20.5%), and G_2/M (21.8%) phases. Similarly normal cell cycle distribution was 57.1% for G_1, 17.7% for S, and 25.1% for G_2/M for MEL290 cells. WA induced G2/M shift in UM cells. G2/M phase shift was more pronounced in MEL290 cells compared to 92.1 cells. A G2/M phase shift was observed at lower concentrations (1.0 μM) of WA treatment but was not present at higher drug concentrations where increasing apoptosis/cell debris was counted in the sub G_0 phase (2.5 and 5.0 μM WA) after 24-h treatment (Fig. 2c). This was associated with a concentration-dependent increased hypodiploid (sub G1) population (Fig. 2d).

The effect of WA on induction of apoptosis in uveal melanoma cells

Flow cytometry studies were performed to evaluate the induction of apoptosis by WA using annexin V/PI co-staining. These results were confirmed by caspase-3 and PARP cleavage on Western blot analysis. An analysis of phosphatidylserine on the outer leaflet of apoptotic cell membranes was performed using annexin V–FITC and PI to distinguish early and late apoptosis from necrosis. UM cells were treated with DMSO, 2.5 μM WA, or 5.0 μM WA for 24 h, and apoptosis was demonstrated in both cell lines in a concentration-dependent manner with a minimal amount of necrosis (less than 5%) (Fig. 3a). In the 92.1 cells, 1% of cells were noted to stain with annexin V indicating early apoptosis, while 21% of cells were dually stained with annexin V and PI indicating a shift toward late apoptosis at 5.0 μM of WA. Conversely, in the MEL290 cells treated with 5.0 μM of WA, early apoptotic effects were observed in 41% of cells, while late apoptosis was observed in 51% cells which was statistically significant compared to controls ($p<0.01$ for both cell lines) (Fig. 3b). Overall, these results exhibited higher sensitivity of MEL290 compared to 92.1 cells to the cytotoxic effect of WA, and confirm trypan blue dye-exclusion assay findings.

To confirm annexin V/PI results, WA-treated cell lysates were evaluated for caspase 3 activation. WA induced caspase 3 activation and PARP cleavage in 92.1 and MEL290 cells in a concentration- and time-dependent manner starting at 1.0 and 2.5 μM in MEL290 and 92.1 cells, respectively (Fig. 3c). We observed that WA induced apoptosis at lower concentrations in MEL290 compared to 92.1 cells after 24-h treatment. These results are consistent with the flow cytometry annexin V/PI data. Overall, these results demonstrated that WA induced apoptosis in 92.1 and MEL290 UM cells.

WA-mediated inhibition of proliferative signaling in uveal melanoma cells

The effects of WA on suppression of c-Met, Akt, and Raf-1 were examined in UM cell lines. WA decreased

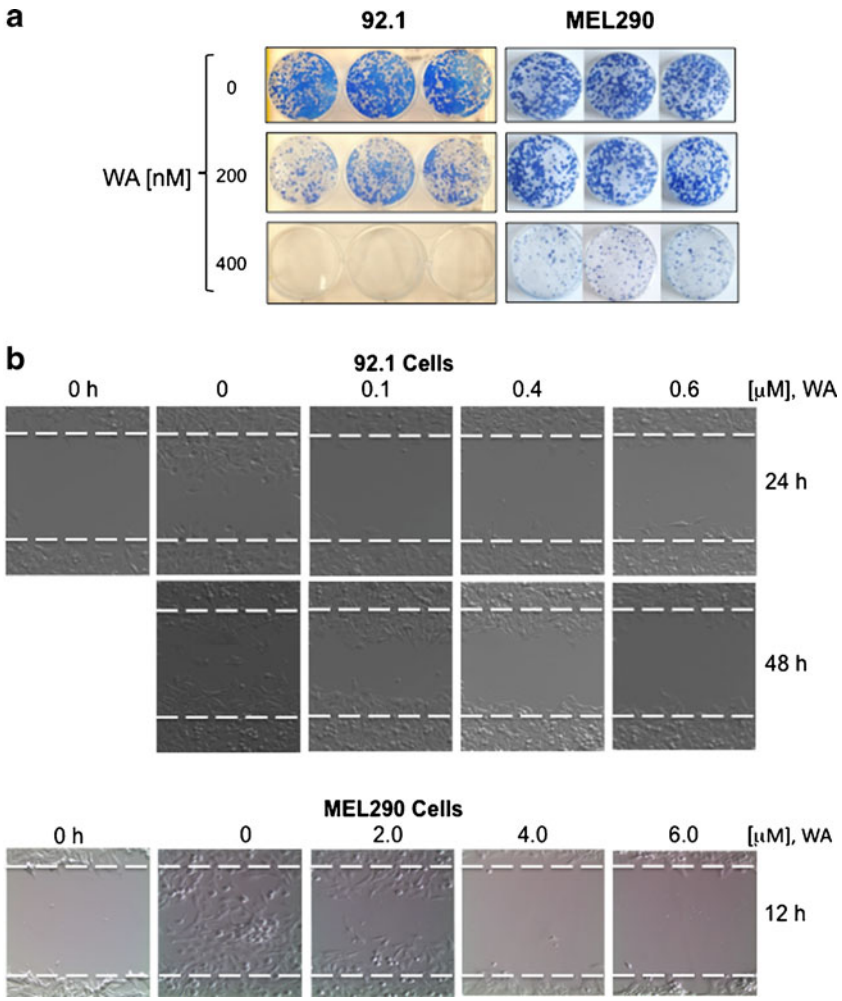

Fig. 2 Clonogenic assay, cell migration and cell cycle analysis. **a** Clonogenic assay shows the long-term effects of WA treatment of human uveal melanoma cells. UM cells treated with DMSO or WA for 24 h as detailed in the Materials and methods; photographs of petri dishes in a representative experiment are shown. **b** Wound healing assay demonstrating inhibition of cell migration of 92.1 cells at 0–0.6 μM after 24 h and Mel290 cells at 0–6.0 μM after 12 h. After cells reach confluence overnight, clear regions were created using sterile pipette tips. After washing, increasing concentrations of WA were added for indicated time. Photographs were taken from representative dishes using phase-contrast microscope. **c** UM cells were treated with increasing concentration of WA for 24 h and stained with propidium iodide and cell cycle analysis was done using flow cytometry. **d** Flow cytometry results demonstrating a concentration-dependent increase in the sub G_1 apoptosis/cellular debris component

phosphorylation of c-Met (Tyr1234) and total levels of c-Met in both 92.1 and MEL290 cells in a concentration-dependent manner. WA activated c-Met at lower concentrations (0.1 and 0.5 μM) in 92.1 cells; however, phosphorylated levels of c-Met were reduced upon treatment with increasing concentrations of WA, whereas total c-Met levels were reduced at all WA-treated concentrations. In contrast, WA decreased c-Met phosphorylation in MEL290 cells in all concentrations of WA examined. Additionally, WA reduced total c-Met levels in both 92.1 and MEL290 cells. WA suppressed Akt (Ser473) phosphorylation and expression of Akt in 92.1 and MEL290 cells (Fig. 4). Expression of Raf-1 was evaluated since 92.1 and MEL290 cells are known to express Raf-1 kinase. In both the 92.1 and MEL290 cells, WA treatment decreased Raf-1 protein levels. 92.1 UM cells' expression of Raf-1 was reduced upon treatment with 0.5 μM of WA while higher concentration of WA (2.5 μM) was required to reduce the expression of Raf-1 in MEL290 cells. Taken together, these results suggest that WA inhibits activation of c-Met and Akt and suppresses expression of c-Met, Akt, and Raf-1 in UM cells.

The effect of WA on UM tumor growth in vivo

To investigate the efficacy of WA on UM in vivo, female SCID mice with a right flank tumor of 92.1 cells were treated with 8 or 12 mg/kg/day of WA or control for 21 days. Representative mice from the control and 8 mg/kg/day

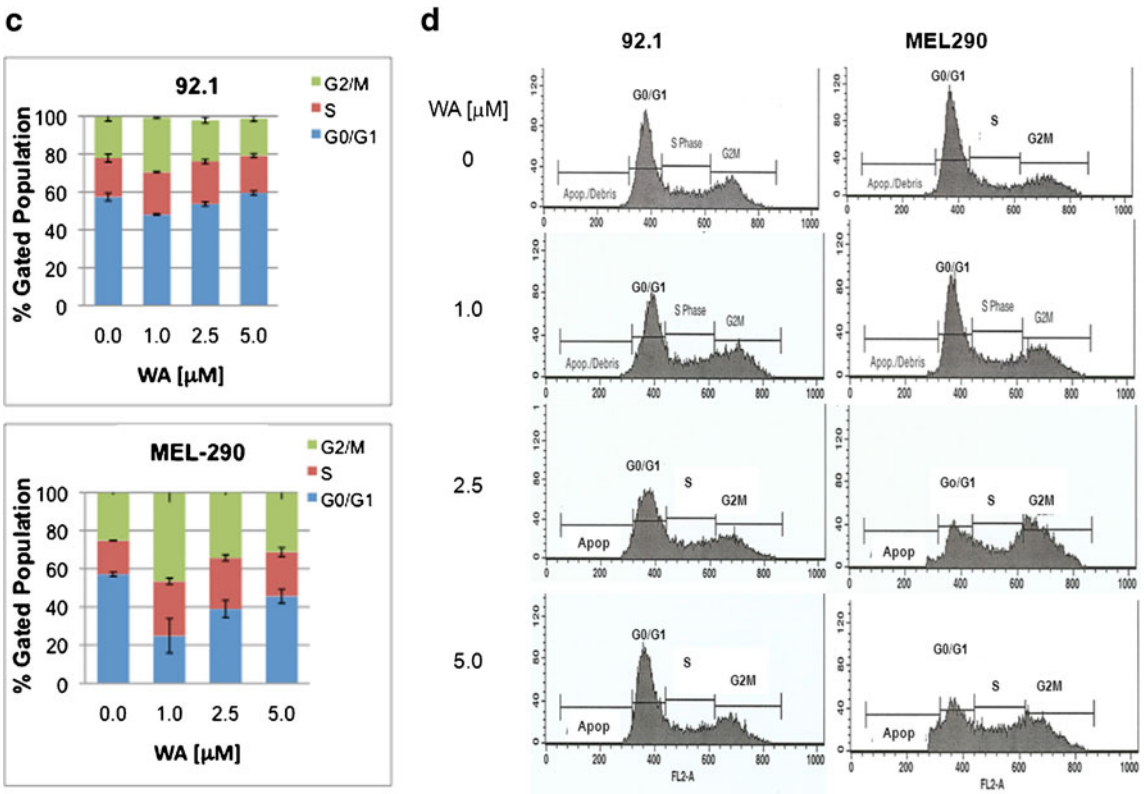

Fig. 2 (continued)

treatment groups were photographed to document the response to WA treatment (Fig. 5a).

In the control group, we observed exponential growth pattern of the tumors in all animals, which reached protocol maximum size (2,000 mm^3) in as early as 30 days post-inoculation. In both treatment groups, there was a decrease in tumor size with treatment (Fig. 5b). For the 8 mg/kg/day group, this inhibition of tumor was observed in 100% of mice with two mice (29%) demonstrating a complete clinical response (CR) to treatment. Another four mice (57%) demonstrated a partial response (PR) to treatment with a greater than 30% tumor reduction, and one animal (14%) demonstrated stabilization of tumor growth (stable disease) by modified RECIST criteria. In the 12 mg/kg/day group, there were three mice (43%) with progressive disease after discontinuation of WA, one CR, one PR, and two additional mice with dose-related toxicity (one having a CR and one with a PR) as noted by marked weight loss and diarrhea with treatment.

At the conclusion of the three-week treatment period and one-month observation period, a significant difference in tumor response to therapy was found between groups as demonstrated by ANOVA (p=0.015). Further analysis was performed comparing the control group to each of the two treatment groups with statistical significance of p=0.004 and p=0.0128 for the 8 mg/kg/day and 12 mg/kg/day treatment groups, respectively. There was no difference in efficacy between the two treatment groups (p=0.173); however, the high-dose group (12 mg/kg/day) demonstrated increased toxicity and mortality compared to the 8 mg/kg/day-group (p=0.03) which mainly consisted of gastrointestinal toxicity. There was a slight decrease in body weight in the animals treated with WA compare to the control group. The high-dose group displayed slightly higher weight lose compared to the low-dose group (Fig. 5c).

Discussion

Withaferin A is a natural withanolide steroidal lactone that has a multi-faceted cytotoxic mechanism of action which is only partially understood. Previous studies have shown its efficacy against multiple tumor types including cutaneous melanoma [5–10]. This is the first evaluation of WA against uveal melanoma demonstrating multiple anti-tumor effects in 92.1, MEL290, and OMM2.3 UM cell lines. These cells carry a ^{WT}BRAF genotype while only the 92.1 cells harbor a GNAQ mutation [31]. In vitro, WA inhibits cell growth with IC50 levels from 1.0 μM to 2.42 μM in the three different UM cell lines showing potency at relatively low concentrations. Control fibroblasts, MRC-5, had an IC50 of 3.81 μM, indicating selective anti-cancer activity of the drug with a

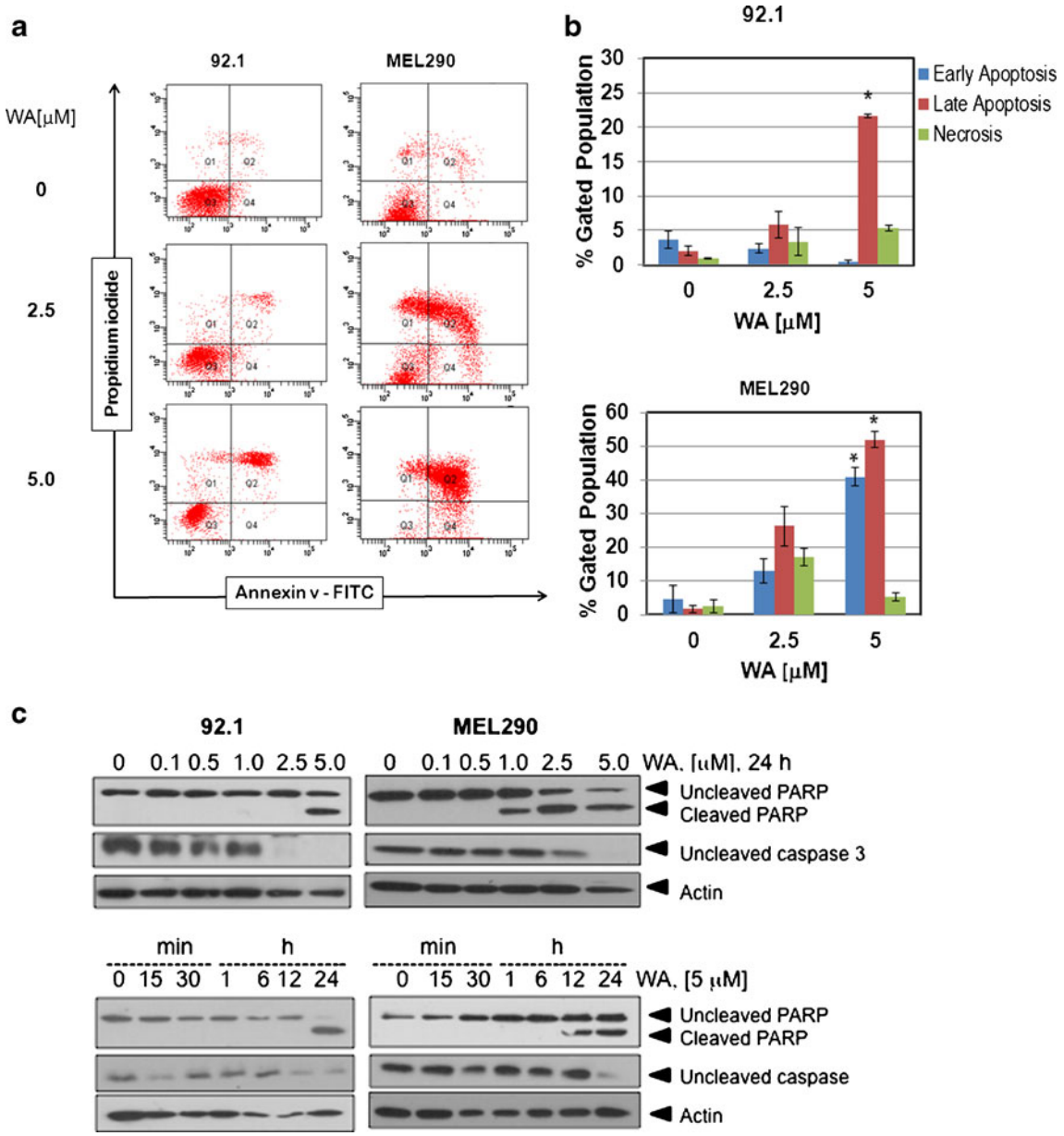

Fig. 3 Effect of WA on induction of apoptosis in UM cells. **a** 92.1 and MEL290 cells were treated with 2.5 or 5.0 μM WA for 24 h. Cells were stained with annexin V/PI and analyzed using flow cytometry. **b** Graphic representation of flow cytometry results showing increased apoptosis with increased concentration of WA. All experiments were performed in triplicate. Results are mean±SD two independent experiments. *$p<0.05$ compared to control cells. **c** WA-mediated induction of apoptosis was determined by treating UM cells with increasing concentration of WA for 24 h or with 5 μM WA for indicated time intervals. In both MEL290 and 92.1 UM cells, WA induced caspase-3 activation and PARP cleavage in a concentration- and time-dependent manner

reasonable therapeutic window. Overall, these results show that WA reduced cell viability and cell proliferation in a concentration- and time-dependent manner in UM cells. Additionally, MEL290 cells are more sensitive to the cytotoxic effect of WA compared to 92.1 cells upon short treatment cycle (Fig. 1b). The results from the colony-forming assay indicate that 24-h WA treatment irreversibly suppressed the colony-forming capacity of UM cells for 10 days even in the absence of the drug. Lack of colony growth with treatment was not reversible after discontinuation of WA treatment, indicating a sustained irreversible anticancer effect of WA on these cells. Furthermore, the cell migration assay demonstrated that nanomolar concentrations of WA inhibited cell migration. Interestingly, while WA suppressed cell migration, a cornerstone capability necessary for tumor invasiveness, this suppression was cell-type specific since 92.1 cells were more sensitive to WA inhibition compared to MEL290 cells.

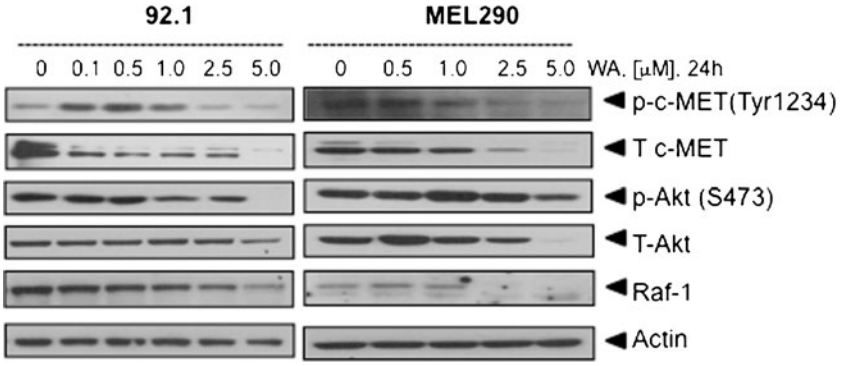

Fig. 4 Effect of WA on pro-survival pathways in UM cells. 92.1 and MEL290 cells were treated with indicated concentration of WA for 24 h. Cell lysates were subjected to Western blot analysis using indicated primary antibodies. These results demonstrated suppression of phosphorylated c-Met and phosphorylated Akt with increasing WA concentration. Furthermore, c-Met and Akt protein levels were reduced. WA reduced c-Met and Akt activation as well as total protein levels in 92.1 and MEL290 cells. Furthermore WA progressively reduced Raf-1 levels in UM cells

Having demonstrated the effect of WA on reduction of cell growth as evidenced by MTS, trypan blue cell exclusion assay, and colony-forming assays, we next explored potential mechanisms of its cytotoxic anti-cancer activity. To confirm prior work, noting cell cycle arrest using WA, we performed cell cycle analysis in 92.1 and MEL290 cells to investigate if a similar effect is observed in UM [9]. Both UM cell lines demonstrated a shift in the cell population from G_1 to G_2/M arrest with WA treatment in a time-dependent manner. When increasing concentrations of WA were evaluated, there was a corresponding increase in hypodiploid sub G_1 population with concurrent G_2/M shift indicating an increase in cell death. To determine if apoptosis contributed to the inhibition of cell growth, we performed annexin V/PI analysis on WA-treated cells. Both UM cell lines had a concentration-dependent induction of apoptosis with increased co-staining of annexin V and PI. These results were confirmed by Western blot analysis, demonstrating cleavage of procaspase 3 and its endogenous substrate PARP at concentrations near the IC50 level of the drug.

We next examined the effect of WA on activation of c-Met as emerging evidence suggests that c-Met is activated in UMs [21, 23, 32]. The c-Met proto-oncogene encodes for the transmembrane receptor tyrosine kinase. Once stimulated, it activates diverse intracellular signaling pathways, including PI3K/Akt, MAP kinase, p38, and signal transducer and activation of transcription 3. It is reported that small molecule inhibitors of c-Met selectively suppress cell proliferation of UM cells [32]. The c-Met ligand, HGF, has also been shown to activate Akt in a c-MET dependent pathway [26]. In our experiments, WA treatment inhibited c-MET phosphorylation and reduced total c-MET protein levels in a concentration-dependent manner in 92.1 and MEL290 cells. The downregulation of c-Met and subsequent loss of its stimulation of downstream events had a significant effect on the survival of UM cells in vitro. Since c-MET potentially plays a role in the metastatic process of UM, targeting this kinase could modulate the metastatic potential of this disease. We demonstrated that WA suppressed the activation of c-Met in 92.1 and MEL290 UM cells and downregulated phospho-AKT protein levels which may contribute to apoptosis in these UM cells. Recent studies have shown that HGF-induced PI3kinase/Akt activation is involved in the migration of UM cells [26]. It is possible that the WA-mediated suppression of UM cell migration observed here may be partly due to downregulation of c-Met and Akt signaling. WA was found to reduce Raf-1 expression in a concentration-dependent manner in both the 92.1 and MEL290 cells. WA appears to affect both the PI3K/Akt and MAP kinase pathways instead of targeting a single protein or pathway.

To determine if these favorable in vitro effects of WA would translate into an animal tumor model, an in vivo efficacy experiment was performed in a UM xenograft model. A flank tumor model was chosen over a liver model because tumors could be directly monitored for growth or regression using a digital caliper. Our xenograft tumors responded to treatment with 100% of animals showing tumor regression or inhibition of tumor growth at the 8 mg/kg/day dose, with 29% having a complete response, and an additional 57% of animals having a partial response to treatment (ANOVA p= 0.015). Both the 8 mg/kg/day and 12 mg/kg/day groups had regression of tumor; however, the 12 mg/kg/day group had increased gastrointestinal toxicity observed during regular monitoring. There was no statistically significant benefit to the 12 mg/kg/day dosing. Although 12-mg/kg/day WA dosing was below the MTD dose for the present model, a lower WA dose is recommended since it reduced tumor mass with no toxicity. Overall, WA demonstrated significant in vivo efficacy against UM tumors. In vitro, WA shows decreased cell

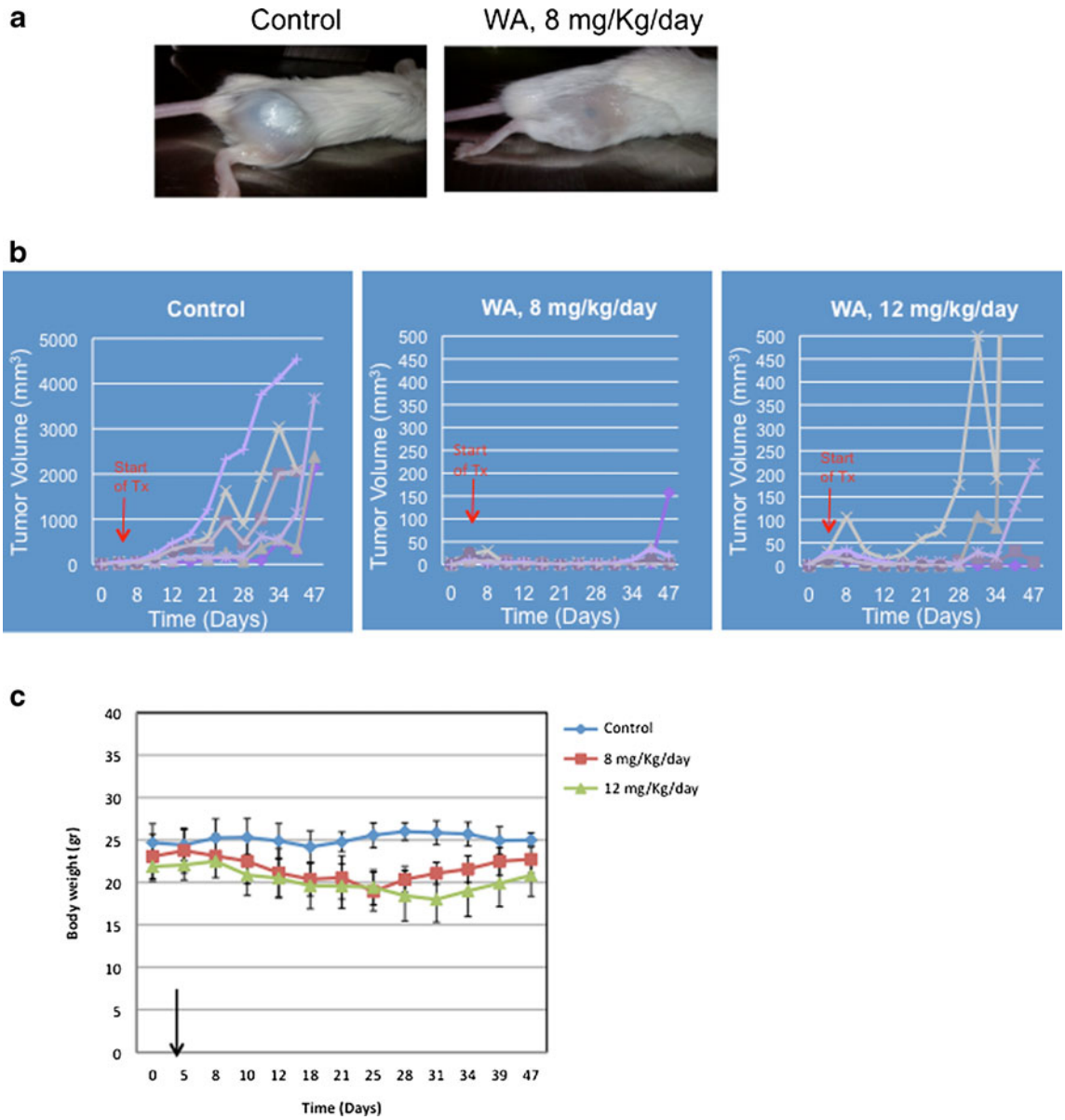

Fig. 5 In vivo model of WA-associated reduction of UM tumor mass. **a** Representative photos from control and WA-treated mice. **b** Tumor growth curves for all three treatment groups showing a marked response to WA treatment. Each line represents an individual animal. **c** Body weight in mice with 92.1 xenografts. The *arrows* indicate the start of treatment

survival, proliferation, colony formation, and cell migration in addition to induction of apoptosis and cell cycle arrest. In vivo, WA demonstrates a substantial reduction of tumor volume and low side effects at the 8 mg/kg/day dose. These data support further translational investigation of WA as a novel therapeutic for this challenging malignancy.

Acknowledgment This work was supported in part by the Kansas Lion's Sight Foundation.

Conflicts of interest None

References

1. Singh AD, Borden EC. Metastatic uveal melanoma. Ophthalmol Clin North Am. 2005;18:143–50.
2. Singh AD, Damato B, Howard P, Harbour JW. Uveal melanoma: genetic aspects. Ophthalmol Clin North Am. 2005;18:85–97.
3. Ven Murthy MR, Ranjekar PK, Ramassamy C, Deshpande M. Scientific basis for the use of Indian ayurvedic medicinal plants in the treatment of neurodegenerative disorders: Ashwagandha. Cent Nerv Syst Agents Med Chem. 2010;10:238–46.
4. Mishra LC, Singh BB, Dagenais S. Scientific basis for the therapeutic use of *Withania somnifera* (ashwagandha): a review. Altern Med Rev. 2000;5:334–46.

5. Choi MJ, Park EJ, Min KJ, Park JW, Kwon TK. Endoplasmic reticulum stress mediates withaferin A-induced apoptosis in human renal carcinoma cells. Toxicol In Vitro. 2011;25:692–8.
6. Lee J, Hahm ER, Singh SV. Withaferin A inhibits activation of signal transducer and activator of transcription 3 in human breast cancer cells. Carcinogenesis. 2010;31:1991–8.
7. Koduru S, Kumar R, Srinivasan S, Evers MB, Damodaran C. Notch-1 inhibition by withaferin-A: a therapeutic target against colon carcinogenesis. Mol Cancer Ther. 2010;9:202–10.
8. Samadi AK, Mukerji R, Shah A, Timmermann BN, Cohen MS. A novel ret inhibitor with potent efficacy against medullary thyroid cancer in vivo. Surgery. 2010;148:1228–36. discussion 1236.
9. Samadi AK, Tong X, Mukerji R, Zhang H, Timmermann BN, Cohen MS. Withaferin A, a cytotoxic steroid from *Vassobia breviflora*, induces apoptosis in human head and neck squamous cell carcinoma. J Nat Prod. 2010;73:1476–81.
10. Samadi A, Loo P, Mukerji R, O'Donnell G, Tong X, Timmermann BN, Cohen MS. A novel hsp90 modulator with selective activity against thyroid cancers in vitro. Surgery. 2009;146:1196–207.
11. Cruz 3rd F, Rubin BP, Wilson D, Town A, Schroeder A, Haley A, Bainbridge T, Heinrich MC, Corless CL. Absence of BRAF and NRAS mutations in uveal melanoma. Cancer Res. 2003;63:5761–6.
12. Kilic E, Bruggenwirth HT, Verbiest MM, Zwarthoff EC, Mooy NM, Luyten GP, de Klein A. The RAS-BRAF kinase pathway is not involved in uveal melanoma. Melanoma Res. 2004;14:203–5.
13. van den Bosch T, Kilic E, Paridaens D, de Klein A. Genetics of uveal melanoma and cutaneous melanoma: two of a kind? Dermatol Res Pract. 2010;2010:1–13.
14. Calipel A, Mouriaux F, Glotin AL, Malecaze F, Faussat AM, Mascarelli F. Extracellular signal-regulated kinase-dependent proliferation is mediated through the protein kinase A/B-Raf pathway in human uveal melanoma cells. J Biol Chem. 2006;281:9238–50.
15. Dhomen N, Marais R. New insight into BRAF mutations in cancer. Curr Opin Genet Dev. 2007;17:31–9.
16. Lefevre G, Babchia N, Calipel A, Mouriaux F, Faussat AM, Mrzyk S, Mascarelli F. Activation of the FGF2/FGFR1 autocrine loop for cell proliferation and survival in uveal melanoma cells. Invest Ophthalmol Vis Sci. 2009;50:1047–57.
17. Palmieri G, Capone M, Ascierto ML, Gentilcore G, Stroncek DF, Casula M, Sini MC, Palla M, Mozzillo N, Ascierto PA. Main roads to melanoma. J Transl Med. 2009;7:86.
18. Onken MD, Worley LA, Long MD, Duan S, Council ML, Bowcock AM, Harbour JW. Oncogenic mutations in GNAQ occur early in uveal melanoma. Invest Ophthalmol Vis Sci. 2008;49:5230–4.
19. Van Raamsdonk CD, Bezrookove V, Green G, Bauer J, Gaugler L, O'Brien JM, Simpson EM, Barsh GS, Bastian BC. Frequent somatic mutations of GNAQ in uveal melanoma and blue naevi. Nature. 2009;457:599–602.
20. Babchia N, Calipel A, Mouriaux F, Faussat AM, Mascarelli F. The PI3k/Akt and mTOR/P70S6K signaling pathways in human uveal melanoma cells: interaction with B-raf/ERK. Invest Ophthalmol Vis Sci. 2010;51:421–9.
21. Mallikarjuna K, Pushparaj V, Biswas J, Krishnakumar S. Expression of epidermal growth factor receptor, ezrin, hepatocyte growth factor, and c-Met in uveal melanoma: an immunohistochemical study. Curr Eye Res. 2007;32:281–90.
22. Hendrix MJ, Seftor EA, Seftor RE, Kirschmann DA, Gardner LM, Boldt HC, Meyer M, Pe'er J, Folberg R. Regulation of uveal melanoma interconverted phenotype by hepatocyte growth factor/scatter factor (HGF/SF). Am J Pathol. 1998;152:855–63.
23. Economou MA, All-Ericsson C, Bykov V, Girnita L, Bartolazzi A, Larsson O, Seregard S. Receptors for the liver synthesized growth factors IGF-1 and HGF/SF in uveal melanoma: intercorrelation and prognostic implications. Invest Ophthalmol Vis Sci. 2005;46:4372–5.
24. Economou MA, All-Ericsson C, Bykov V, Girnita L, Bartolazzi A, Larsson O, Seregard S. Receptors for the liver synthesized growth factors IGF-1 and HGF/SF in uveal melanoma: intercorrelation and prognostic implications. Acta Ophthalmol. 2008;86:20–5.
25. Peruzzi B, Bottaro DP. Targeting the c-Met signaling pathway in cancer. Clin Cancer Res. 2006;12:3657–60.
26. Ye M, Hu D, Tu L, Zhou X, Lu F, Wen B, Wu W, Lin Y, Zhou Z, Qu J. Involvement of PI3k/Akt signaling pathway in hepatocyte growth factor-induced migration of uveal melanoma cells. Invest Ophthalmol Vis Sci. 2008;49:497–504.
27. Abdel-Rahman MH, Yang Y, Zhou XP, Craig EL, Davidorf FH, Eng C. High frequency of submicroscopic hemizygous deletion is a major mechanism of loss of expression of PTEN in uveal melanoma. J Clin Oncol. 2006;24:288–95.
28. Saraiva VS, Caissie AL, Segal L, Edelstein C, Burnier Jr MN. Immunohistochemical expression of phospho-Akt in uveal melanoma. Melanoma Res. 2005;15:245–50.
29. Mitsiades N, Chew SA, He B, Riechardt AI, Karadedou T, Kotoula V, Poulaki V. Genotype-dependent sensitivity of uveal melanoma cell lines to inhibition of B-Raf, MEK, and Akt kinases: rationale for personalized therapy. Invest Ophthalmol Vis Sci. 2011;52:7248–55.
30. Casagrande F, Bacqueville D, Pillaire MJ, Malecaze F, Manenti S, Breton-Douillon M, Darbon JM. G1 phase arrest by the phosphatidylinositol 3-kinase inhibitor LY 294002 is correlated to up-regulation of p27Kip1 and inhibition of G1 CDKs in choroidal melanoma cells. FEBS Lett. 1998;422:385–90.
31. Harbour JW, Onken MD, Roberson ED, Duan S, Cao L, Worley LA, Council ML, Matatall KA, Helms C, Bowcock AM. Frequent mutation of *BAP1* in metastasizing uveal melanomas. Science. 2010;330:1410–3.
32. Abdel-Rahman MH, Boru G, Massengill J, Salem MM, Davidorf FH. MET oncogene inhibition as a potential target of therapy for uveal melanomas. Invest Ophthalmol Vis Sci. 2010;51:3333–9.